Aerodynamic Dispersion of Anode Arc Attachment Through a Converging–Diverging Nozzle

He-Ji Huang, Wen-Xia Pan, and Cheng-Kang Wu

Abstract—Electrode ablation is a key factor that affects the life and performance of the direct current arc plasma generator, which is closely related to the near-electrode behavior of the arc. Compared with the constricted-type arc root, diffused-type arc root is more conducive to reduced thermal load, thereby improving the electrode life and the discharge stability. The attachment behavior of the arc root is related to the transport properties of the arc near the electrode wall and the aerodynamic and electromagnetic forces on the root of the arc. From this point of view, aerodynamical dispersion of the arc root using a converging–diverging nozzle was proposed, and the key factors that affect the dispersion were analyzed and verified.

Index Terms—Aerodynamical dispersion, arc plasma generator, diffused arc root attachment.

NOMENCLATURE

Primary Symbols

A	Area.
C	Specific heat.
C_d	Drag coefficient.
E	Energy.
F	Force.
I	Current.
j	Current density.
M	Mach number.
m	Mass flowrate.
p	Pressure.
ρ	Density.
r	Radius.
T	Temperature.
U	Voltage.
V	Volume.
υ	Velocity.
γ	Ratio of specific heats.
η	Efficiency.
θ	Angle.

μ_0	Vacuum permeability.
φ	Polar angle.

Notations

0	Initial/edge/wall value.
$*$	Critical value.
c	Arc column.
cond	Conduction.
d	Dynamic.
drag	Drag.
e	Expansion.
ero	Erosion.
in	Input.
max	Maximum value.
mean	Mean value.
r	Radial direction.
rad	Radiation.
s	Statistic.
t	Throat/total.
z	Axial direction.

I. INTRODUCTION

THE increase of the number and scale of technical applications of arc plasma leads to more stringent requirements on the reliability of the process [1]. Among various influencing factors, thermal-induced electrode erosion is a key one. Electrode erosion not only leads to shorter lifetime of the plasma torch but also deteriorates the quality of the plasma process in a relatively uncontrollable way, which significantly reduces the cost–performance ratio. Looking back over the past decades of arc plasma torch developments, we can see that a continuous effort was devoted to improve the electrode erosion performance [2], [3].

From an energy balance consideration, the erosion rate of a certain volume of electrode material lying under the hot spot of an arc root can be written as

$$V_{\text{ero}} = \frac{E_{\text{in}} - E_{\text{cond}} - E_{\text{rad}}}{\rho C \, \Delta T}. \qquad (1)$$

Equation (1) means that if the input energy (E_{in}) could not be fully dissipated by the sum of thermal conduction (E_{cond}) and radiation (E_{rad}), there must be some material removal (V_{ero}) due to the temperature increase ΔT great enough to evaporate the material to maintain the energy balance. Among all the variables on the right hand of (1), E_{in}, which is proportional to j^2, might have the largest adjustable range.

This article has been accepted for inclusion in a future issue of this journal. Content is final as presented, with the exception of pagination.
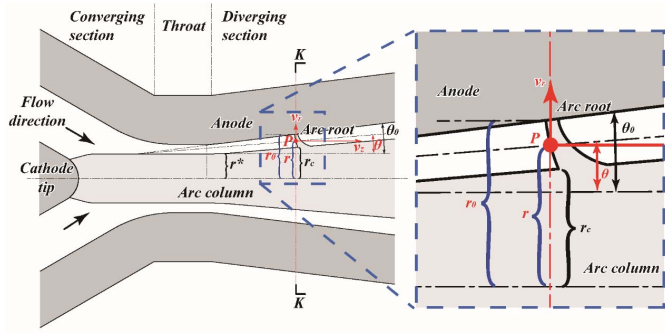
2

IEEE TRANSACTIONS ON PLASMA SCIENCE

Fig. 1. Illustration of a nontransferred direct current plasma in a conical-shaped CD nozzle configuration. A partial enlarged view of the arc root (right).

Fig. 2. (a) Anode arc attachment in a parabolic shape. (b) Schematics of the arc attachment on the $K–K$ plane.

As j is defined by

$$j = \frac{I}{A}. \tag{2}$$

There are two ways to reduce j by either reducing current I or enlarging the arc attachment area A. The former could be realized by operating the arc plasma torch at a high-voltage and low-current mode, usually be possible with the addition of an interelectrode channel to elongate the arc length [4]–[6]. While for the latter one, either a rapid moving arc or a splitted electrical discharge could enlarge the temporal-averaged A [7]–[11]. On the other hand, a stable but real diffusion attachment with transient larger A is more desirable. This is because the moving arc might lead to high-frequency fluctuations which hinder its application in the advanced industry where high controllability is required.

However, although a diffusion attachment is observable in cases such as those when argon or natural gas (propane butane) exists [12], [13] or where a "hot" anode [14] is present, the mechanism of the diffusion attachment is still not clear.

Based on a qualitative understanding, the formation of a diffusion attachment is the result of the balance between the z-pinch of the arc root and the energetically favorable arc root shape and position following Steenbeck's principle of minimum power in gas discharge [15]. Both higher electrode temperature and plasma gas with higher electrical conductivity promote the electrical conductivity in the boundary layer, which reduces the energy barrier for arc breakdown, facilitating diffusion attachment. From this point of view, we propose a mechanism of arc root dispersion by improving the effect of aerodynamic expansion using a converging–diverging (CD) nozzle.

II. THEORETICAL ANALYSIS AND RESULTS

Fig. 1 illustrates the part of a nontransferred direct current plasma in a CD nozzle near the throat. The proposed CD nozzle is in a conical shape, and the whole nozzle also acts as the anode. The cathode is inserted into the converging cavity. The expansion half-angle of the diverging part is θ_0. A constricted anode attachment of the arc root is shown here for the theoretical analysis.

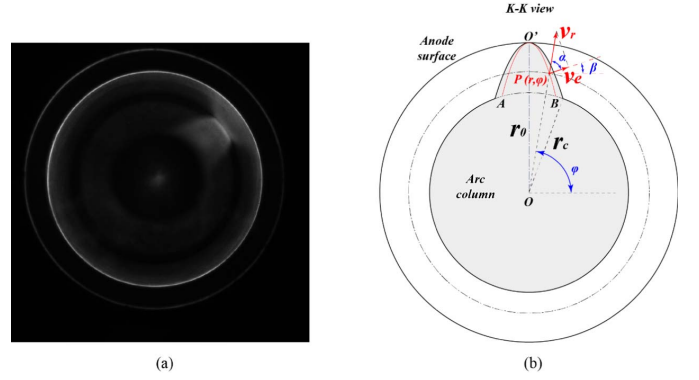When the plasma flows through the throat and enters the diverging section, it will expand due to the pressure difference between the nozzle inlet and outlet. The expansion angle θ of the flow varies at different radial positions. For point P on the arc column, it seems to be reasonable to assume that

$$\theta = \frac{r - r^*}{r_0 - r^*}\theta_0 \tag{3}$$

where r is the radial position of point P, r^* is the radius of the arc column in the throat, and r_0 is the radius of the nozzle channel on the cross-sectional view of $K–K$, as illustrated in Figs. 1 and 2(b). Equation (3) assumes that the flow near the central axis does not expand much, while the expansion angle of the peripheral flow increases gradually until it equals θ_0 at the nozzle inner wall. Such an expansion leads to a radial component of the flow velocity $\vec{v}_r = \vec{v}_z \tan\theta$.

Fig. 2 shows the schematic arc root attachment on $K–K$ plane. Previous research shows that when the arc root attachment is a constricted one in a weakly expanded channel, it shows a parabolic shape of the arc column near the anode surface [8], as shown in Fig. 2(a). The plasma was generated at the arc current of 80 A. The 10 vol% H_2–Ar with total gas flow rates of 8.6 slm was used as a plasma gas. The chamber pressure was kept at 10 kPa. In Fig. 2(b), the radial velocity $\vec{v}_r$ will have another component of $\vec{v}_e$, which is normal to the parabola $AO'B$ at point P. From the geometry relationship between vector components, the ratio of $\vec{v}_e$ to the main flow velocity $\vec{v}$ at point P is deduced as

$$\frac{\vec{v}_e}{\vec{v}_z} = \tan\left(\frac{r_s - ab}{1 - ab}\theta_0\right)\cos\left[\varphi - \arctan\left(-\frac{1}{2}\frac{b}{kr_t r_s \cos\varphi}\right)\right] \tag{4}$$

where $r_s = (r/r_0)$ is the radius position normalized by the nozzle radius. The coefficients are $a = (r^*/r_t)$, $b = (r_t/r_0)$, and $k = -(r_0 - r\sin\varphi/r^2\cos^2\varphi)$. Note that $\vec{v}_z$ is a function of position r, $\vec{v}_z = \vec{v}_z(r)$. For a given point P with coordinates of (r_p, φ_p), the parabola of $AO'PB$ is determined by

$$r\sin\varphi = k_P r^2 \cos^2\varphi + r_0. \tag{5}$$

From (4), the ratio of v_e/v_z is calculated for discrete points in the parabola region, as shown in Fig. 3(a) and (b). Fig. 3 shows the distributions of v_e/v_z on the up-right quarter of the $K–K$ view, as illustrated in Fig. 2(b). In this example, θ_0 equals 7° and the relative arc column size is 70% of the whole channel ($a = 0.7$). Following the assumption in (3),

This article has been accepted for inclusion in a future issue of this journal. Content is final as presented, with the exception of pagination.

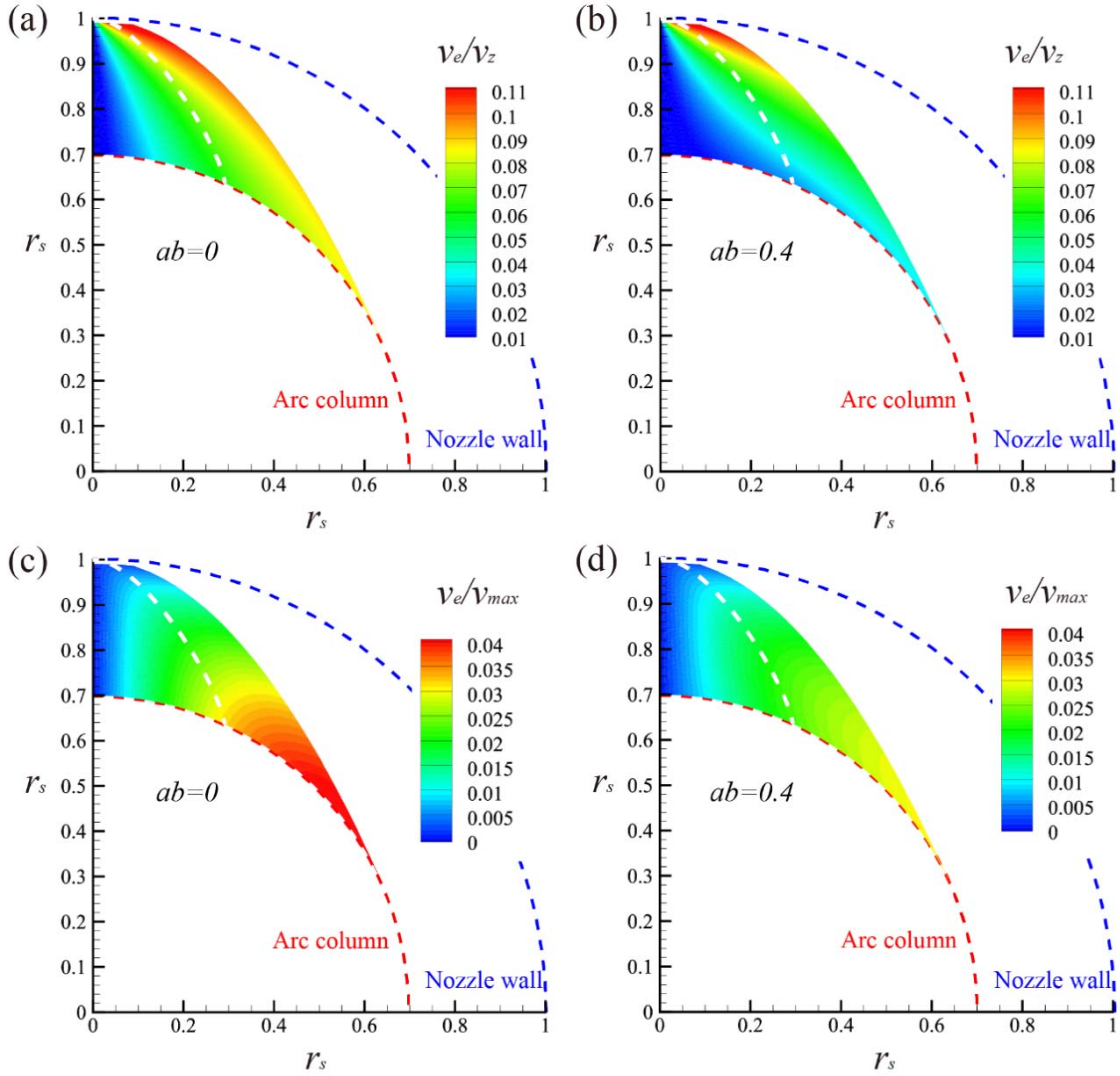HUANG *et al.*: AERODYNAMIC DISPERSION OF ANODE ARC ATTACHMENT THROUGH A CD NOZZLE

3

Fig. 3. Component v_e distributions in the parabolic region where $\theta_0 = 7°$. (a) and (c) $ab = 0$. (b) and (d) $ab = 0.4$. (c) and (d) v follows a parabolic distribution.

for a larger ab ($ab = r*/r_0$), the value of component v_r is smaller, which is more pronounced near the arc column center. Fig. 3(a) and (b) shows the comparison of $ab = 0$ and 0.4, respectively. When the considered point is closer to the parabolic axis of symmetry, the direction of $\bar{v}_r$ is also closer to the tangential direction, resulting in a smaller normal component of $\bar{v}_e$, which is clearly shown in Fig. 3.

If the main velocity also follows a parabolic distribution radially, which is usually consistent with the experimental results, that is, $v_z = v_{max}(1 - r_s^2)$. When the flow is axisymmetric, $v_{max} = 2v_{mean}$, thus (4) can be rewritten to

$$\frac{v_e}{v_{mean}} = 2(1 - r_s^2) \tan\left(\frac{r_s - ab}{1 - ab}\theta_0\right)$$
$$\times \cos\left[\varphi - \arctan\left(-\frac{1}{2}\frac{b}{kr_tr_s\cos\varphi}\right)\right]. \quad (6)$$

Fig. 3(c) and (d) shows the distribution of v_e/v_{max}, which is the result of a counterbalance between the value of v and v_r/v.

In order to realize the dispersion of the arc root, the aerodynamic drag force should be large enough to overcome the pinch effect caused by the electromagnetic force and to expand

and push the arc column region close enough to the anode surface to achieve breakdown. The aerodynamic drag force

$$F_{drag} = p_d C_d A_a. \quad (7)$$

The dynamic pressure p_d

$$p_d = \frac{1}{2}\rho v^2 = \frac{1}{2}p_s \gamma M^2. \quad (8)$$

Based on the relationships between p_s and p_t, ρ_s and ρ_t, and T_s and T_t for compressible flows [16], together with the mass conservation equation, p_d can be rewritten to

$$p_d = \frac{1}{2}\frac{\dot{m}}{A}\sqrt{\gamma RT_t}M\left(1 + \frac{\gamma - 1}{2}M^2\right)^{\frac{-1}{2}}. \quad (9)$$

Let $K_d = M(1 + (\gamma - 1/2)M^2)^{(-1/2)}$. Fig. 4 shows the dependence of K_d on M for various γ. It shows that K_d increases with M, and the effect of γ is quite small at low M conditions. When M is less than 0.5, K_d increases almost linearly with M. This is because although (8) suggests that p_d increases with M^2, the statistic pressure p_s drops rapidly at higher flow velocity. Therefore, the portion of the
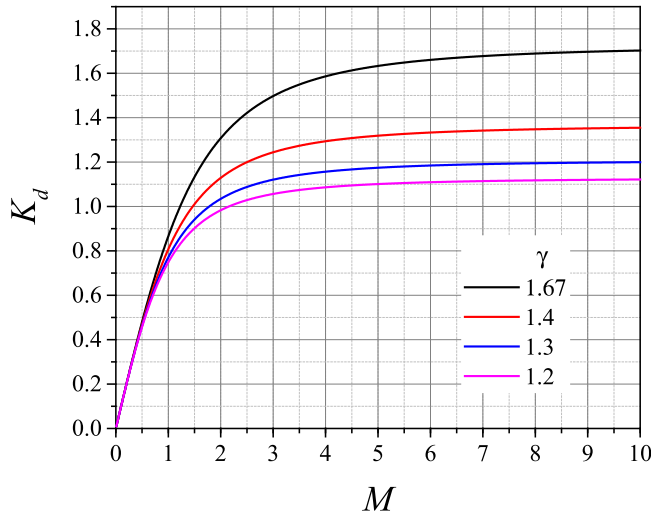
This article has been accepted for inclusion in a future issue of this journal. Content is final as presented, with the exception of pagination.

4

IEEE TRANSACTIONS ON PLASMA SCIENCE

Fig. 4. Dependence of K_d on M for various γ.

Fig. 5. Proposed 3-D arc column geometry near the anode surface.

expansion component of the drag force is similar to that shown in (4) and (6)

$$\frac{p_{de}}{p_d} = 2(1 - r_s^2) \tan\left(\frac{r_s - ab}{1 - ab}\theta_0\right)$$
$$\times \cos\left[\varphi - \arctan\left(-\frac{1}{2}\frac{b}{kr_t r_s \cos\varphi}\right)\right]. \quad (10)$$

From the expression of K_d, it is shown that when M is much greater than 1, K_d approaches the value of $(\gamma - 1/2)^{(-1/2)}$. This is because with certain enthalpy level, the dynamic pressure has its maximum when all the energies have been converted to kinetic energy, which will never exceed the total energy of the flow.

The total temperature is contributed by two parts: the cold flow temperature and the temperature rise due to the electric power input. It can be written as

$$T_t = \eta\frac{IU}{C_p \dot{m}} + T_0. \quad (11)$$

When the plasma exists, since $T_0/T_t \ll 1$, T_0 could be neglected, and therefore (8) is approximated to

$$p_d = \frac{1}{2A}\sqrt{IU\dot{m}\eta(\gamma - 1)}K_d. \quad (12)$$

Although (12) is only valid for calorically perfect gas, when the change of γ is taken into account, it can be used for approximate estimations with acceptable error range at low Mach number cases (e.g., $M < 2$).

To simplify the estimation of the z-pinch effect of the arc attachment, all the cross sections perpendicular to $\vec{j}$ are assumed to be in circular shapes, as shown in Fig. 5. In this case, if current I is in the parabolic distribution, the z-pinch pressure of a point of the arc column in a circular cross section of radius r_z equals

$$p_z = \frac{5}{3}\frac{\mu_0}{4\pi}\frac{I^2}{2\pi r_z^2(1 - \sin\varphi_0)}\left(1 - \frac{12}{5}\frac{r_1^2}{r_z^2} + \frac{9}{5}\frac{r_1^4}{r_z^4} - \frac{2}{5}\frac{r_1^6}{r_z^6}\right). \quad (13)$$
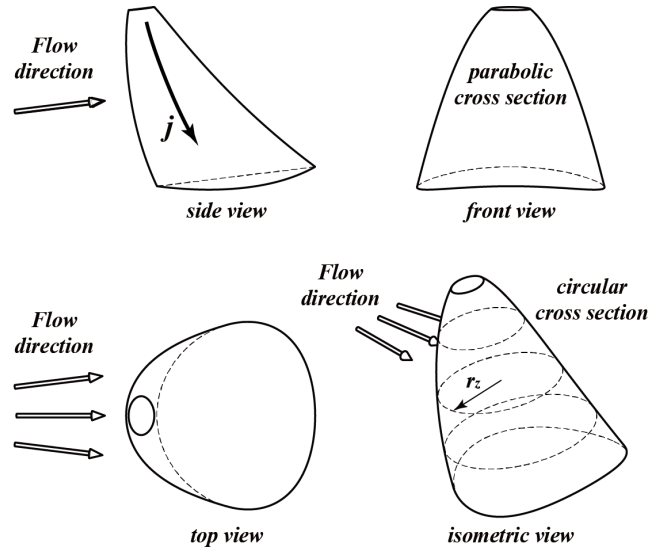
Here, $r_1 = r\cos\varphi$, and φ_0 represents the position of the arc column edge.

From the combination of (10), (12), and (13), it shows that the proportional relationship between the z-pinch pressure and the expansion component of dynamic pressure is

$$\frac{p_z}{p_{de}} \propto \frac{\mu_0 I^2}{\sqrt{IU\dot{m}\eta}}\frac{1}{K_d} \quad (14)$$

which suggests that the arc column tends to expand at higher gas flow rates, higher Mach number, and higher power input efficiency, while with higher arc current, the z-pinch effect is more pronounced.

Fig. 6(a)–(d) shows the effect of M on (p_z/p_{de}) with other parameters the same as those illustrated in Fig. 3. The dark region in Fig. 6 shows p_z being greater than p_{de}. However, this does not mean that the arc column inside will not expand, because the z-pinch pressure itself is somewhat already balanced by the pressure caused by the temperature difference between the inner and outer arc columns. The extra p_{de}, even if it is smaller than p_z, also causes the arc column near the anode surface to expand. The light gray parts shown in Fig. 6 are p_z being smaller than p_{de}. Within this region, the arc will swell rapidly, especially at the outer edge. Once the edge of the arc column expands to such a position that the breakdown voltage V_b is smaller than the original voltage drop V_o (as illustrated in the inset of Fig. 6), a wider arc attachment will form and eventually get a diffusion attachment. In Fig. 6, it is clearly shown that M plays an important role for the dispersion of the arc root. When M increases from 0.01 to 0.6, the area of p_{de} larger than p_z increases from 6.8% to 51.7%.

Some preliminary experimental results have been shown in [17]. Using a torch with $r_t = 3$ mm and $\theta_0 = 5°$, N_2 plasma was generated in vacuum at flow rates among 4.5–30 slm. A self-designed copper mirror with weak-reflecting material imbedded at the center part was used to observe the condition of the arc root attachment on the anode surface. The images of the arc root attachments were recorded by an intensified charge coupled device camera at an exposure time of 5 μs. The

This article has been accepted for inclusion in a future issue of this journal. Content is final as presented, with the exception of pagination.

HUANG *et al.*: AERODYNAMIC DISPERSION OF ANODE ARC ATTACHMENT THROUGH A CD NOZZLE 5
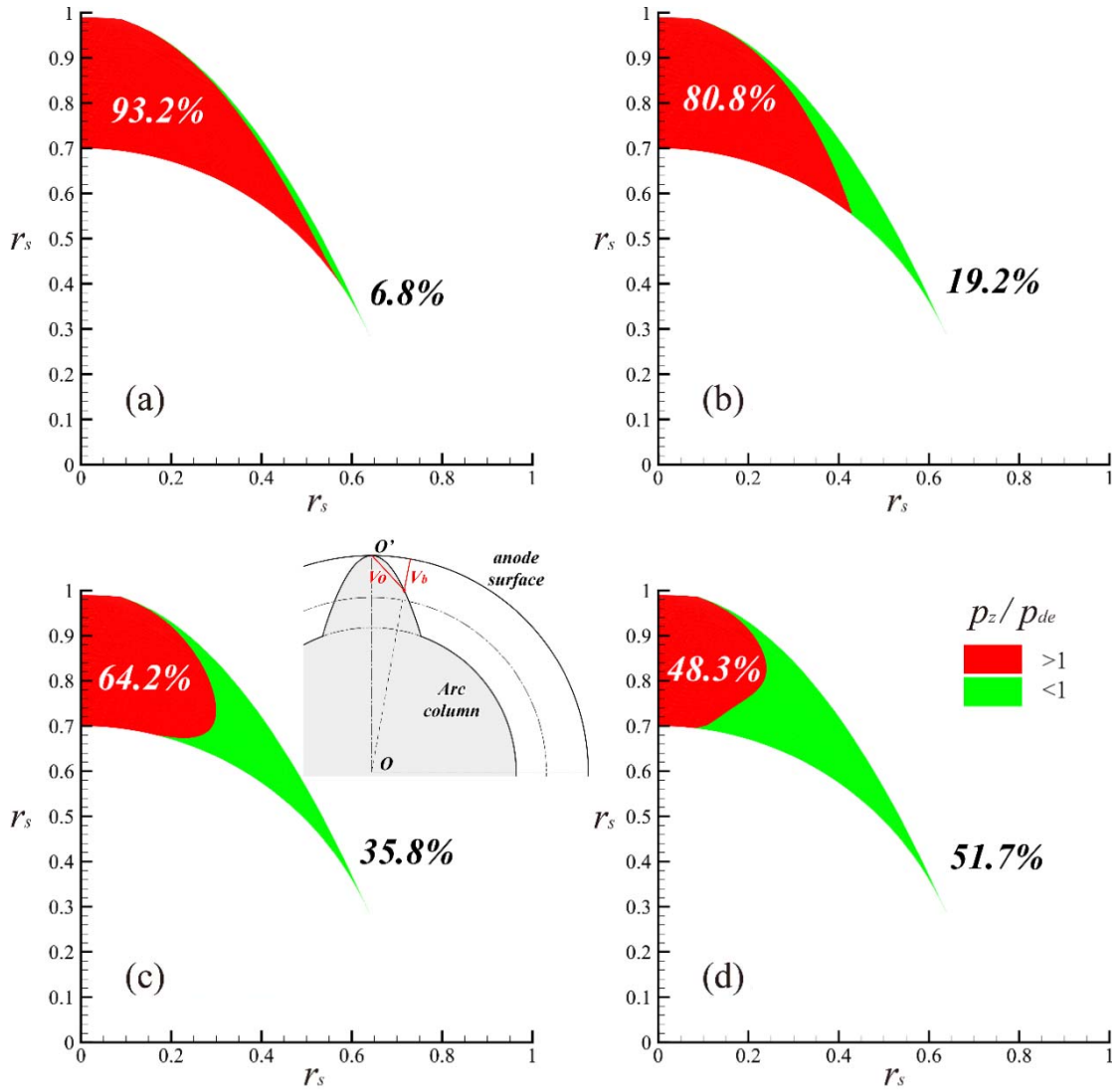

Fig. 6. Effect of M on the ratio of p_z/p_{de}. (a) $M = 0.01$. (b) $M = 0.1$. (c) $M = 0.3$. (d) $M = 0.6$.

TABLE I
EXPERIMENTAL PARAMETERS AND THE OBSERVED TRANSITION OF ARC ATTACHMENT TYPES

I (A)	U (V)	$\dot{m}$ (kg/s)	$\dfrac{\mu_0 I^2}{\sqrt{IU\dot{m}}}$	p_c (Pa)	Arc attachment type
120	25	0.12E−03	2.96E−02	50	constriction
140	45	0.14E−03	2.58E−02	74	transition
140	55	0.18E−03	2.08E−02	85	diffusion

transition from constriction to diffusion arc attachment is seen when the total plasma gas flow rate increases. Table I shows the discharge parameters and the corresponding observed arc root attachment types. Although M was not measured in the experiment, a higher M and thus K_d at elevated gas flow rate is expected, because the pressure in the cathode cavity p_c increases. It is shown that when the dimensionless value of $(\mu_0 I^2/(IU\dot{m})^{1/2})$ decreases from 2.96E−2 to 2.08E−2,

the arc attachment type changes from constriction to diffusion one.

III. CONCLUSION

Above results suggest that it is possible to achieve a diffusion arc attachment by optimizing the geometry parameters of the CD nozzle, such as the throat size and the expansion angle. To get a desired M large enough for the dispersion of

the anode arc root attachment, or with a certain CD nozzle configuration, a combination of the discharge parameters can also affect the arc attachment type. A dimensionless parameter of $(\mu_0 I^2/(IU\dot{m})^{1/2})$ could be utilized to estimate the arc attachment type in present experimental conditions.

REFERENCES

[1] M. F. Zhukov and I. M. Zasypkin, *Thermal Plasma Torches: Design, Characteristics, Applications*. Cambridge, U.K.: Cambridge International Science Publishing, 2007.

[2] Y. Wu, "Visualization and mechanisms of splashing erosion of electrodes in a DC air arc," *J. Phys. D: Appl. Phys.*, vol. 50, no. 47, p. 47LT01, Nov. 2017.

[3] M. Tanaka, T. Hashizume, K. Saga, T. Matsuura, and T. Watanabe, "Diode-rectified multiphase AC arc for the improvement of electrode erosion characteristics," *J. Phys. D: Appl. Phys.*, vol. 50, no. 46, p. 465604, Oct. 2017.

[4] M. Gindrat, R. K. Schmid, R. Molz, and D. Hawley, "Recent and advanced techniques to increase reliability and life of torches in the thermal spray industry," in *Proc. 3rd Int. Round Table Thermal Plasmas Ind. Appl.*, Muldersdrift, South Africa, 2011, p. 71.

[5] W. Pan, X. Meng, C. Wu, and X. Chen, "Experimental study on the thermal argon plasma generation and jet length change characteristics at atmospheric pressure," *Plasma Chem. Plasma Process.*, vol. 26, no. 4, pp. 335–345, Aug. 2006.

[6] W. Pan, Z. Y. Guo, X. Meng, H. J. Huang, and C. K. Wu, "Fluctuation characteristics of arc voltage and jet flow in a non-transferred dc plasma generated at reduced pressure," *Plasma Sour. Sci. Technol.*, vol. 18, no. 4, p. 045032, Oct. 2009.

[7] J. P. Trelles, "Computational study of flow dynamics from a dc arc plasma jet," *J. Phys. D: Appl. Phys.*, vol. 46, no. 25, p. 255201, Jun. 2013.

[8] H.-J. Huang, W. X. Pan, and C. K. Wu, "Arc root motions in an argon–hydrogen direct-current plasma torch at reduced pressure," *Chin. Phys. Lett.*, vol. 25, no. 11, p. 4058, Nov. 2008.

[9] L. C. Li, W. D. Xia, H. L. Zhou, Z. P. Zhou, and B. Bai, "Experimental observation and numerical analysis of arc plasmas diffused by magnetism," *Eur. Phys. J. D*, vol. 47, no. 1, pp. 75–81, Apr. 2008.

[10] O. M. Chumak, A. Mašláni, and Hrabovský, "Experimental observations of arc-anode attachment in steam-argon-air environment," in *Proc. 12th High-Tech Plasma Process. Conf.*, vol. 406, 2012, p. 012009.

[11] J. Schein, J. Zierhut, M. Dzulko, G. Forster, and K. D. Landes, "Improved plasma spray torch stability through multi-electrode design," *Contrib. Plasma Phys.*, vol. 47, no. 7, pp. 498–504, Nov. 2007.

[12] M. Auweter-Kurtz, H. L. Kurtz, and S. Laure, "Plasma generators for re-entry simulation," *J. Propuls. Power*, vol. 12, no. 6, pp. 1053–1061, 1996.

[13] P. Wenxia, M. Xian, L. Teng, C. Xi, and W. Chengkang, "Comparative observation of Ar, Ar-H_2 and Ar-N_2 DC arc plasma jets and their arc root behaviour at reduced pressure," *Plasma Sci. Technol.*, vol. 9, no. 2, p. 152, Apr. 2007.

[14] W. Pan, H. Huang, and C. Wu, "Effect of nozzle temperature on the performance of a 1 kW H_2-N_2 arcjet thruster," *Plasma Sci. Technol.*, vol. 12, no. 4, pp. 473–477, 2010.

[15] H.-P. Li, E. Pfender, and X. Chen, "Application of Steenbeck's minimum principle for three-dimensional modelling of DC arc plasma torches," *J. Phys. D: Appl. Phys.*, vol. 36, no. 9, pp. 1084–1096, Apr. 2003.

[16] AMES Research Staff, "Equations, tables, and charts for compressible flow," Ames Aeronautical Lab., Moffett Field, CA, USA, Tech. Rep. 1135, 1953.

[17] W. Pan, L. Chen, X. Meng, Y. Zhang, and C. Wu, "Sufficiently diffused attachment of nitrogen arc by gasdynamic action," *Theor. Appl. Mech. Lett.*, vol. 6, no. 6, pp. 293–296, Nov. 2016.